MAIN LECTURES

ML-01
ENGINEERED INTERFACE-INTERPHASE SYSTEMS ON AUTOMOTIVE POLYOLEFINES SURFACE AND THEIR INFLUENCE ON ADHESION

W. (VOYTEK) S. GUTOWSKI*, SHENG LI, ALEX BILYK, and IKO BURGAR

CSIRO Division of Materials Science & Engineering Functional Interphases & Coatings and Intelligent Materials Team, Graham Road (PO Box 56), Melbourne, Highett, Victoria 3190, Australia
Voytek.Gutowski@csiro.au

Abstract

Significant adhesion enhancement of various surface-finishing materials to chemically inert automotive polyolefin blends can be attained through surface grafted connector molecules reactive with oxidized substrate surface. The effectiveness of adhesion improvement through such tethered interfaces is shown to depend on the mode of interaction with the adjacent medium: interpenetration or chemical reaction, as well as surface density and length of grafted molecules.

We have frequently observed that some systems, such as painted or otherwise decoratively coated products, fail through the delamination of the coating from the substrate surface at the stress levels well below the anticipated load-bearing capacity of the tethered interface. Two hypotheses have been formulated to explain the observed phenomenon:

(i) The chain scission in surface oxidized polyolefins takes place not only in the uppermost polymer surface, but may propagate into the sub-surface region, thus creating a weak boundary layer which fails cohesively through its bulk,

(ii) In order to increase the load-bearing capacity of the interphase, the sub-surface region of the substrate needs to be reinforced by short-chain molecules penetrating into and subsequently providing effective crosslinks between individual fragments of excessively oxidized and hence, weaker sub-surface part of the interphase.

In this paper we fully verify the above hypotheses. The oxidized sub-surface layer reinforced by polyethyleneimine becomes an integral part of the effective interphase in addition to the tethered interface and the interpenetrated network of connector molecules and the paint.

Possibility of lignin application in rubber blends based on NR and SBR was studied. Seven types of lignin powder were tested as fillers for rubber blends before and after modification. Influence of lignin on vulcanisation process, mechanical properties, morphological structure as well as dynamical-mechanical properties was investigated. The significant positive effect of modified lignin on properties of model rubber blends was found.

ML-02
POLYMER NANOTECHNOLOGY APPLIED TO POLYMER ALLOYS AND COMPOSITES

TOSHIO NISHI* and KEN NAKAJIMA

WPI Advanced Institute for Materials Research, Tohoku University, 2-1-1 Katahira, Aoba-ku, Sendai 980-8577 Japan
nishi.toshio@wpi-aimr.tohoku.ac.jp

Introduction

Recently, there have been many attempts to develop nano-structured polymeric materials to satisfy the ever-increasing demand of the automotive and electronics industry to accommodate a green and sustainable society. This demand requires such materials to be multi-functional and high performance. Therefore, research and development into structure optimization and related processing development for polymer alloys and polymer-based composites have become more important subjects because single polymeric materials can never satisfy such requirements. This situation accelerates the development of evaluation techniques that have nanometer-scale resolution[1]. To date, transmission electron microscopy (TEM) has been widely used for this purpose. However, TEM technique cannot probe the mechanical properties of such materials in general. The realization of much higher performance materials requires an evaluation technique that enables us to investigate topological and mechanical properties at the same point and the same time. Atomic force microscopy (AFM)[2] is clearly an appropriate candidate because it has almost comparable resolution with TEM. Furthermore, mechanical properties can be readily obtained by AFM due to the fact that the sharp probe tip attached to the soft cantilever directly touches on the surface of the materials in question. Therefore, many polymer researchers have started to use this novel technique to characterize materials properties at the nanoscale[3].

However, there are several drawbacks in AFM usage for soft materials such as polymeric and bio-related materials[4]. For example, the sample deformation caused by the force between the probe tip and the sample can lead to mistaken interpretation of the obtained topography as explained later. The phase contrast image obtained together with the topography image using the so-called tapping-mode is difficult to interpret or provides at most qualitative information. We have been engaged for many years in using AFM with a sufficient understanding of its advantage and disadvantage in order to develop methodology suitable for polymeric soft materials, namely, nanorheology[5] and nanotribology[6,7]. The peculiar feature of these methods is the positive usage of sample deformation, a feature which becomes troublesome in imaging. We are able to extract mechanical information on polymeric materials from the physical quantity, sample deformation. Due to this fact, we may refer to this method as a nano-palpation technique, where a doctor's finger is replaced by the sharp

AFM probe tip. In order to realize this idea, analyses of force-distance curves have proven to be powerful, and correspond to macroscopic stress-strain curves. In the analysis, sample deformation and force exerted are quantitatively estimated to acquire a true topographic image free from the effect of sample deformation together with a Young's modulus image[8] and an adhesive energy image[9] at the same time. In this paper, we applied this method to dynamically vulcanized thermoplastic elastomer (TPE-V) system and newly manufactured non-viscoelastic polymer alloy (NOVA).

Method

As mentioned above, the sample deformation caused by direct touch of the AFM sharp probe is inevitable in AFM usage. If this effect is negligible, an obtained image expresses a true surface topography. However, soft-materials such as polymers and biomaterials are easily deformed even by a very weak force. For example, a 0.1–10 nN force exerted by a 10 nm-diameter punch probe results in a stress of 1.3–130 MPa. Plastic materials with having a GPa-order Young's modulus might not be deformed significantly by this range of force, whereas rubbery materials with a MPa-order modulus and gels with a kPa-order modulus undergo substantial deformation. The sharper the probe tip, the more serious is this effect.

Does this effect become a disadvantage or an advantage? This question can lead to different answers depending on the researcher's viewpoint. In this chapter, our answer is an advantage; we can measure the surface Young's modulus because of this effect. Instrumentation to obtain a measure of "hardness" by pushing some kind of probe onto a surface began their history with a hardness indenter tester and the main stream of recent progress is seen in the nano-indenter system[10]. The recently-developed nano-indenter can provide two-dimensional mechanical mapping, though the lateral resolution achieved is far below that of the AFM. The advantage of the indenter compared to the AFM is: *i*) the probe shape is geometrically similar and therefore the analysis is easier; *ii*) the material of the probe is diamond and thus it has no elastic deformation and is free from wear; *iii*) the force-detection system is independent of the displacement-detection system. In contrast, AFM uses the deflection of the cantilever for the force detection. The sample deformation is also measured from the conversion of this quantity, resulting in a fundamental difficulty in analyzing the mechanical properties of materials. Probes coated with diamond-like carbon are now commercially available, but there remain several problems such as durability and controllability of probe shape. On the other hand, there exist disadvantages in indenter systems. The indenter probes are designed to record plastic deformation from the instant of contact and therefore it becomes difficult to combine a two-dimensional mapping capability. The force range is in the order of μN to mN, not comparable to pN or nN as realized in AFM. In the case of AFM, almost all probes have effective roundness at the top of the probe tip except for a carbon-nanotube (CNT)-attached probe, resulting in measurement in the elastic deformation region below the yield limit. Thus, a two-dimensional mapping capability is easily realized by AFM-based indentation. Like body palpation by medical doctors or masseurs, we can now perform nano-palpation with the AFM sharp probe enabling measurement of surface elasticity.

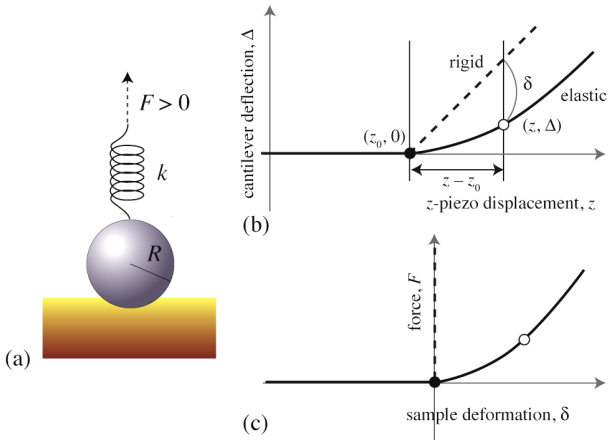

Fig. 1. **Analysis procedure of force-distance curve with and without adhesive force between sample and AFM probe.** (a) The schematics of the contact between two bodies when the applied force is positive (repulsive), (b) the force-distance curve for the contact without adhesive interaction, (c) the corresponding force-deformation plot

The simplest theory for the analysis of surface elasticity based on AFM force-distance curve measurement is Hertzian contact mechanics[11]. As schematically shown in Fig. 1, a force-distance curve is a plot of the displacement, z of the piezoelectric scanner normal to the specimen's surface as the horisontal axis and the cantilever deflection, Δ as the vertical axis. Hertzian contact mechanics cannot treat adhesive force in principle. We need to make some effort to minimize the adhesive force in a practical experiment. Measurement in aqueous conditions is effective for polymeric materials with low water absorbability. A cantilever with a larger spring constant also hides weak van der Waals forces. Fig. 1a shows the force-distance curve measurement on soft-materials during the loading process. The AFM cantilever and probe are treated as a spring with a spring constant of k and a sphere with radius of curvature, R, respectively. The force is expressed by Hooke's law,

$$F = k\Delta \qquad (1)$$

Since recent developments in this field have included several reports on direct measurement of k and R,[12–14] it is expected to realize improved quantitative accuracy.

If the specimen surface is sufficiently rigid, the cantilever deflection, Δ always coincides with the displacement, $(z - z_0)$ of the piezoelectric scanner measured from a contact point $(z_0, 0)$ as depicted in the dashed line in Fig. 1b. However, if the specimen surface undergoes elastic deformation as in the case of the solid line, we can estimate the sample deformation, δ as follows;

$$\delta = (z - z_0) - \Delta \qquad (2)$$

δ-F plot, shown in Fig. 1c, derived from the $z - \Delta$ plot is now fitted with the theory of Hertzian contact to provide the estimated Young's modulus,

$$a=\left(\frac{FR}{K}\right)^{1/3},\ \delta=\left(\frac{F^2}{K^2R}\right)^{1/3}\quad \therefore F=KR^{1/2}\delta^{3/2} \tag{3}$$

where a is contact radius and K is so-called elastic coefficient and expressed using reduced Young's modulus E^* as follows,

$$K\equiv\frac{4}{3}E^*=\frac{4}{3}\left[\frac{1-\nu_s^2}{E_s}+\frac{1-\nu_p^2}{E_p}\right]^{-1} \tag{4}$$

where E_i and ν_i are Young's modulus and Poisson's ratio, respectively. The subscript suffix i stands for sample (s) and probe (p).

AFM is widely used in the world as an imaging tool for soft-materials like polymers and biomaterials. Contact and tapping-mode operations are known as major imaging modes. Specimens are scanned over their surfaces with mechanical contact in both modes. Thus, it has been said among researchers that topographic images from both modes are affected by the deformation of the sample itself due to contact or tapping forces. The users might be also able to qualitatively understand the influence of a contact or tapping forces for obtained topographic images in the past. However, the imaging with constant force condition never results in quantitative estimation of such influences.

Now, here will be demonstrated the quantitative method to obtain accurate topographic images of deformable samples together with Young's modulus distribution images. Especially, our interest in this paper exists in soft-materials that are commonly difficult for AFM to deal with. The final goal is to understand peculiar properties of soft-materials, i.e., mechanical and rheological properties at nano-meter scale. The value of a cantilever spring constant, k is an important factor to detect mechanical properties from a sample surface as mentioned above. If k is very small, the cantilever approaching to the surface cannot deform the sample. If k is very large, instead, the cantilever can deform the sample, without any deflection. Therefore, necessary information about the sample is lacking. Thus, we need to choose a cantilever with an appropriate value for k.

To obtain the mapping of the local mechanical properties of soft-materials, force-volume (FV) measurement would be the most appropriate method. In this mode, force-distance curve data are recorded until a given cantilever deflection value (trigger set-point), Δ_{trig} is attained for 64 × 64 (or 128 × 128 for the latest condition) points over two-dimensional surface. At the same time, z-displacement, z_{trig} corresponding to the trigger set-point deflection was recorded to build an apparent topographic image. The topographic image taken in this mode is basically same from that by conventional contact mode if contact force set-point and trigger set-point are identical. If all the points over the surface are rigid enough, the set of recorded displacements, z_{trig} represents the topographic feature (true height) for the sample. However, if the surface deforms as discussed, it is no more valid to regard an obtained data as the real topographic information. However, since we have a force-distance curve for each point, we can estimate the maximum sample deformation value for each point referring to Eq. (*2*),

$$\delta=\left(z_{trig}-z_0\right)-\Delta_{trig} \tag{2}$$

Then, two-dimensional arrays of sample deformation value can be regarded as sample deformation image. The force-distance curve analyses for 4,096 or 16,384 data give the sets of Youngs modulus distribution images at the same time and the same place. We now have apparent height (z_{trig}) and sample deformation (δ) images taken at the same time and Δ_{trig} is the preset value and therefore constant for all of force-distance curves. Then, the appropriate determination is performed for contact point (the array of (z_0, 0)), this realizes the reconstruction of "true" surface topography free from sample deformation[8].

Results & Discussion

During dynamic vulcanization process, thermoplastic matrix materials as well as rubber components are generally blended in an extruder resulting in so-called co-continuous morphology. A cross-linking agent can be also added into the extruder. During the cross-linking of the rubber-rich phase the viscosity of the rubber increases, which results in the increased blends viscosity ratio, since the viscosity of the thermoplastic matrix remains the same. The shear stress causes rubber-rich phase to break up into fine dispersed rubber particles in a thermoplastic matrix. The formation of the characteristic matrix-particle morphology is essentially influenced by the kinetics of the vulcanization and the cross-linking density of the rubber phase[15,16]. Due to the nanometer-scale dispersion, TPE-V, thus, can be regarded as one of the most promising polymer nano-alloys.

If the cross-linking density of the rubber phase is very poor, the phase will be able to undergo large deformation and remains co-continuous. On the other hand, if the cross-linking

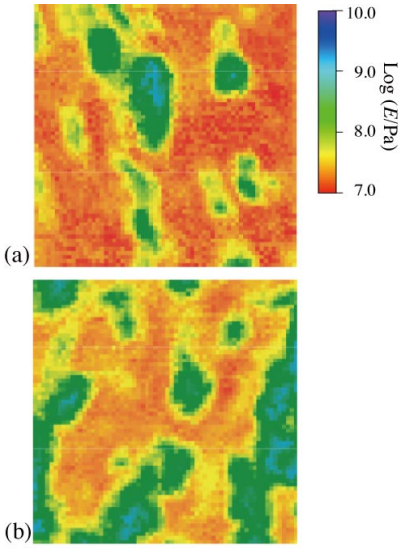

Fig. 2. **Young's modulus mappings of crystalline EVA/EVA rubber 3:7 reactive blend.** The scan size was 2 μm. (a) without dynamic vulcanization and (b) with dynamic vulcanization

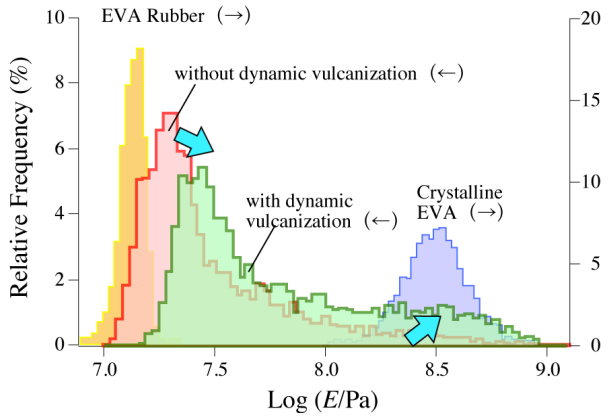

Fig. 3. **Young's modulus distribution obtained from Fig. 1.** The distribution for each pure component is also superimposed

density is too high, the rubber phase can only be deformed under shear stress without ripping. Therefore an optimum of cross-linking density should exist. To date, there have been many researches conducted to elucidate the complicated dynamic vulcanization process. However, many of researches only treated structural information obtainable by microscopic techniques together with macroscopic mechanical property testing. Here, we introduce the results obtained by our nano-mechanical mapping for a TPE-V specimen. TPE-V specimens were prepared as follows[17]; A vinyl silane was firstly grafted on rubbery ethylene vinyl acetate copolymer (EVA rubber) to obtain silylated rubber. Then, the product was mixed with crystalline EVA in a twin-screw extruder. The masterbatch was put in a mixer with or without cross-linking catalyst to realize dynamic vulcanization.

Fig. 2 shows the Young's modulus mapping images for crystalline EVA/EVA rubber 3:7 reactive blend. As explained above, EVA rubber is designed to be cross-linked if cross-linking catalyst exists in the vulcanization process. Fig. 2a is for the blend without dynamic vulcanization and 2b is for that with dynamic vulcanization. In the case of Fig. 2a, the see-island structure was observed. However, as one can see from Young's modulus distribution shown in Fig. 3, both phases had the modulus different from their pure constituents. This was attributed to the fact that this blend system was composed of partially miscible polymers. Especially, crystalline EVA rich phase perfectly lost crystalline hardness (~GPa). On the other hand, dynamically vulcanized sample showed co-continuous structure that could not be expected from original blend ratio. In addition, Fig. 3 indicated two important findings. The first one was the increase of Young's modulus in rubber rich phase. This could be easily explained as the consequence of the vulcanization of EVA rubber. The second, more interesting one was the recovery of crystalline hardness in the crystalline EVA rich phase. We speculated that this was due to vulcanization-induced phase separation. This kind of observation cannot be realized by TEM or even by conventional AFM.

Another application example of this technique is non-viscoelastic polymer alloy (NOVA)[18]. This materials shows soft response to high-speed input which never be explained by conventional idea of viscoelasticity. We performed this technique to pursue the mechanism of this strange property. Fig. 4 shows the apparent height and Young's modulus images of NOVA manufactured by twin-screw extruder with L/D=100. NOVA is composed of a certain resin and a certain rubber and rubbery phases are dispersed at nano-meter scale. The manner of dispersion is essentially same as other polymer-based nano-alloys looking at Fig. 4a, while Young's modulus image implied us a very interesting phenomena. The hollows in apparent height image (of course due to pressure by AFM sharp probe) correspond to rubber-rich phases. Then, the matrix phase is corresponding to resin-rich phase. However, in the Young's modulus image, intermediate phases appear where the Young's modulus is lower than that of matrix. Furthermore, this intermediate phase appears as co-continuous phase. The existence of intermediate phase could not be observed for other nano-dispersed polymer alloy systems and it is uniquely observed in NOVA. More detailed discussion will be made at the site.

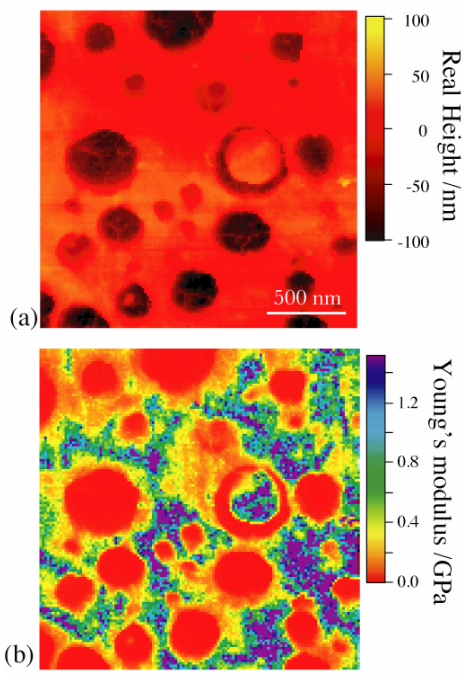

Fig. 4. **(a) apparent height and (b) Young's modulus images of NOVA.** The scan size was 2 μm. The intermediate phase is clearly visible in Young's modulus image

We thank for the financial support from New Energy Development Organization (NEDO) as one of the projects in the Nanotechnology Program by the Ministry of Economy, Trade, and Industry (METI) of Japan.

REFERENCES

1. Nishi T., Nakajima K.: *Kobunshi Nano Zairyo,* (Kobunshi Gakkai, ed.). Kyoritsushuppan, Tokyo 2005.
2. Binnig G., Quate C. F., Gerber Ch.: Phys. Rev. Lett. *56*, 930 (1986).
3. Magonov S. N., Whangbo M. H.: *Surface Analysis with STM and AFM*. VCH, Weinheim 1996.

4. Nakajima K., Fujinami S., Nukaga H., Watabe H., Kitano H., Ono N., Endoh K., Kaneko M., Nishi T.: Kobunshi Ronbunshu *62*, 476 (2005).
5. Nakajima K., Yamaguchi H., Lee J. C., Kageshima M., Ikehara T., Nishi T.: Jpn. J. Appl. Phys. *36*, 3850 (1997).
6. Terada Y., Harada M., Ikehara T., Nishi T.: J. Appl. Phys. *87*, 2803 (2000).
7. Komura M., Qiu Z., Ikehara T., Nakajima K., Nishi T.: Polym. J. *38*, 31 (2006).
8. Nukaga H., Fujinami S., Watabe H., Nakajima K., Nishi T.: Jpn. J. Appl. Phys. *44*, 5425 (2005).
9. Nagai S., Fujinami S., Nakajima K., Nishi T.: Compos. Interf. *16*, 13 (2009).
10. Oliver W. C., Pharr G. M.: J. Mater. Res. *7*, 1564 (1992).
11. Landau L., Lifchitz E.: *Theory of Elasticity*. Mir, Moscow 1967.
12. Butt H. J.: J. Colloid Interface Sci. *180*, 251(1996).
13. Hutter J. L., Bechhoefer J.: Rev. Sci. Instrum. *64*, 1868 (1993).
14. Wang T., Ikai A.: Jpn. J. Appl. Phys. *38*, 3912 (1999).
15. Radusch H.-J., Pham T.: Kautsch. Gummi Kunstst. *49*, 249 (1996).
16. Abdou-Sabet S., Puydak R. C., Rader C. P.: Rubber Chem. Technol. *69*, 476 (1996).
17. Sugita K., Watanabe K., Inoue T.: to be published.
18. Inoue T.: to be published.

ML-03
POTENTIALS OF RUBBER NANO-COMPOSITES IN AUTOMOTIVE APPLICATIONS

KATHARINA BRANDT, HAGEN LORENZ, LUCIANE KLAFKE DE AZEREDO SCHNEIDER, and ROBERT H. SCHUSTER

Deutsches Institut für Kautschuktechnologie e. V., Eupener Str. 33, 30519 Hannover
Robert.schuster@dikautschuk.de

Introduction

For technical and ecological reasons there is nowadays a keen interest in saving oil resources and translating into action innovative concepts for efficient engines and global CO2 reduction. For the rubber technology the urgent challenges are to use more conscious the raw materials. Taking into consideration that reinforcing fillers used in the rubber industry are oil based and/or produced by high energy consumption processes one urgent demand is to develop strategies for alternative fillers made from natural sources. In these regards, it has been recognized that natural nano-fibers and natural occur-ring plate-like fillers have the potential to play a similarly graded role alongside conventional filler. The present contribution is meant to introduce new concepts for *in-situ* manufacturing of Cellulose, Rubber/Cellulose and Rubber/Clay-nanocomposites, respectively as well as for polymeric nano-particles. Morphological features and physical properties of the corresponding rubber nanocomposites will be discussed in the following.

Methodology

Cellulose nano-fibers are *in-situ* formed by applying the "continuous dynamic latex compound-ding" (CDLC) proprietary process based on a co-coagulation of cellulose xanthate and rubber latex (NR, SBR, NBR, ACM) in an elongation flow jet. Rubber/clay nano-composites are obtained by submitting aqueous slurry of pristine montmorillonite and rubber latex to an elongational/turbulent flow followed by coagulation. Morphological investigations were performed on vulcanized composites by TEM, XRD, AFM. Standard mechanical properties, dynamic cut growth resistance, swelling and permeation of model fuel were measured.

Results and discussion

A more unexplored field is the reinforcement by short and long nano-fibers. Rubber composites containing *in-situ* formed cellulose nano-fibers display an opposite behavior to composites containing carbon black, silica and polymeric nano-particles. By applying the CDLC technique the fibers are well incorporated and dispersed in the rubber matrix and do not show an agglomeration and flocculation tendency during storage of unmodified mixes. The high aspect ratio (130–250) and fiber density increases with the elongational flow prior to co-coagulation. In addition the cellulose fibers can be linked to the rubber matrix by covalent bonds. As a result the composites relax shortly after the breakdown of the storage modulus during an amplitude sweep (non-linear viscoelasticity). The recovery of 95–98 % of the initial properties is unique for elastomer nano-composites. The large solid-rubber interface is probed by a larger reduction of equilibrium swelling than the one shown by silica and carbon black at constantφ. The specific fiber network formed at relatively low concentrations lead to dynamic-mechanical properties which are superior to those of generated by silica and carbon black at the same loading (Fig. 2). The reinforcing effect can be explained by accuring an effective aspect ratio of ca. 20. The results show. That the reinforcement obtained by silica can be achieved by employing only half volume fraction of *in-situ* formed cellulose fibers. The same beneficial effects can be reported for tensile properties whre anisotropic effects come into function for calendared nanocomposites.Considering rubber/clay nanocomposites obtained without any modification of MMT by the new CDLC process well dispersed and partly fanned out (intercalated?) factoids be-

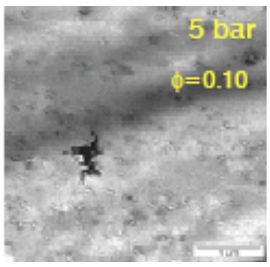

Fig. 1. ***In-situ* formed cellulose fibres**

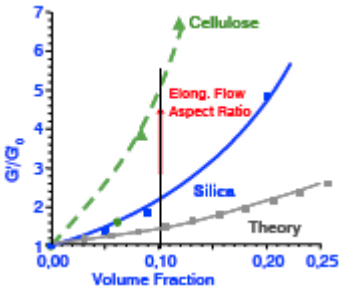

Fig. 2. **Normalized storage modulus as a function of φ,** 1) Cellulose, 2) Silica, 3) Guth-Gold prediction

come obvious from TEM and XRD investigations (Fig. 3). This underlines the advantages of the CDLC process which is short, effective, requires less energy than mechanically mixing and is inexpensive. The improvement of the mechanical properties level increases significantly in nano-composites produced by CDLC compared to composites obtained by melt mixing. The polarity of the rubber matrix however plays an important role. As far barrier properties are concerned, the reduction of permeation coefficient reduction by 51 % generated by a volume fraction 0.04 MMT is in accordance to theoretical expectations for an aspect ratios of ca. 50.

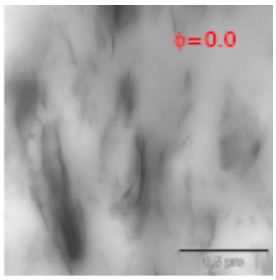

Fig. 3. **Morphology of rubber/MMT**

Conclusion

New processing techniques permit the use of new and competitive types of fillers. The polymeric fillers, long and short nanofibers as well as well dispersed plate-like fillers offer a reliable base to reduce conventional properties of the elastomers.

ML-04
LANXESS - INNOVATIVE SOLUTIONS FOR SUSTAINABLE ECONOMIC GROWTH

FLEMMING B. BJOERNSLEV

LANXESS Central Eastern Europe s.r.o., Chief Executive Officer, Štetinova 4, 811 06 Bratislava, Slovak Republic
flemming.bjoernslev@lanxess.com